

Retrieval of Vertical Profiles of Cirrus Cloud Microphysical Parameters from Doppler Radar and Infrared Radiometer Measurements

S. Y. MATROSOV

Cooperative Institute for Research in Environmental Sciences, University of Colorado/NOAA, Boulder, Colorado

B. W. ORR, R. A. KROPFLI, AND J. B. SNIDER

NOAA/Environmental Technology Laboratory, Boulder, Colorado

(Manuscript received 25 January 1993, in final form 1 November 1993)

ABSTRACT

This paper describes a new method to retrieve vertical profiles of the parameters of cirrus cloud microphysics that are important for the estimation of climatic feedback. These parameters are the particle characteristic size and ice mass content. The method also allows calculations of vertical profiles of particle concentrations and ice mass flux. The method uses measurements of radar reflectivities and Doppler velocities from the ground-based zenith-viewing radar combined with measurements of downwelling brightness temperatures from an infrared radiometer operating in the "window" (10–12 μm) region. The proposed method is illustrated on data obtained on 26 November 1991 during FIRE-II [First ISCCP (International Satellite Cloud Climatology Project) Regional Experiment] in Coffeyville, Kansas. This paper also presents estimates of uncertainties of parameter retrieval due to different a priori assumptions about particle shapes, distributions, fall velocity–size relationships and due to errors in measurements. Comparisons with in situ measurements showed reasonable agreement.

1. Introduction

It is widely recognized that high-altitude cirrus clouds play an important role in the planetary radiation budget (Stephens et al. 1990). Such clouds are located in the upper troposphere and composed mostly of ice particles of different shapes. Parameterization of cirrus clouds remains a problem for general circulation models (GCM) because the magnitude and sign of their climatic impact depend heavily on the characteristic particle sizes and ice mass content (IMC). Various combinations of sizes and ice water path (which is the vertical path integral of IMC usually abbreviated as IWP) could produce feedbacks in GCMs that are different in magnitude and sign (Ebert and Curry 1992).

Uncertainties in modeling cirrus cloud properties dictate a need for remote sensing techniques to gather information about microstructural parameters of such clouds. Existing techniques for estimating ice cloud microphysical parameters usually employ at least two different remote sensors, or spectral measurements at different wavelengths. This is because the radiation (measured by radiometers) and backscattering (measured by lidars and radars) depend on both particle sizes and concentrations. Different combinations of

these parameters can produce the same signal measured by one of the sensors but not both simultaneously.

It should be mentioned that there are a number of empirical relationships between IMC and radar reflectivities (e.g., Sassen 1987; Liao and Sassen 1992). These relationships, however, are based on simultaneous calculations of IMC and reflectivities for measured particle spectra and represent only average relationships without accounting for independent variations of particle sizes and concentrations.

Techniques based on radiometer measurements provide vertically averaged information about cloud parameters (e.g., Parol et al. 1991) due to the nature of these measurements. Estimation of vertical profiles requires making assumptions about vertical distributions of the desired parameters. For some applications, like GCMs with the vertical resolution in the upper troposphere of about 1–2 km, the vertically averaged characteristic particle sizes and IWP values in cirrus clouds could be the most appropriate information to use. However, vertical profiles of radiatively important cloud parameters (i.e., characteristic sizes and IMC) can provide a better understanding of cloud structure and development.

Estimating vertical profiles of cloud parameters requires vertically resolved measurements like those provided by radars and lidars. Intrieri et al. (1993) proposed an approach to infer effective radii of assumed spherical ice particles from the ratio of radar and CO_2

Corresponding author address: Sergey Y. Matrosov, CIRES/NOAA ETL 325 Broadway, R/E/ET6, Boulder, CO 80303.

lidar backscatter. This approach, however, has its limitations. Greatly separated in wavelengths, radar and lidar sometimes see cloud boundaries differently (Uttal and Intrieri 1993). Attenuation of lidar signals in ice clouds complicates the retrieval and even makes it impossible for relatively dense cirrus clouds.

In an earlier paper, Matrosov et al. (1992) proposed a technique for estimating IWP and characteristic particle size averaged vertically through the cloud from combined ground-based measurements of radar reflectivities and IR brightness temperatures in the atmospheric "window," 10–12 μm . In this paper, a further development of this technique is proposed and demonstrated with data taken with the Wave Propagation Laboratory (WPL) Doppler Ka-band radar during FIRE-II [First ISCCP (International Satellite Cloud Climatology Project) Regional Experiment] in Coffeyville, Kansas, in 1991. The unique element here is the use of vertical profiles of Doppler velocities and radar reflectivities to infer vertical profiles of particle characteristic sizes and IMC. Possible errors in retrieved parameters due to assumptions made about shape and size distributions of cirrus cloud particles are also evaluated.

2. Theoretical background

Radar backscattering depends on two principal parameters of cloud microstructure, that is, particle characteristic size and concentration, which vary greatly within the cloud. Thus, one measurement of radar reflectivity at each range gate is insufficient to find these two parameters. In addition to reflectivity, however, Doppler radar also provides an additional measurement at each range gate, that is, Doppler velocities. Measured Doppler velocities V_m represent the sum of reflectivity-weighted particle fall velocities V_f and of vertical air motion V_a :

$$V_m = V_f + V_a. \quad (1)$$

For the purpose of this paper, it is V_f that is of interest and not V_a . Later in the paper, an averaging procedure used to eliminate V_a and to estimate particle fall velocities is described. For now it is assumed that two vertical profiles are known, that is, vertical profiles of radar reflectivity Z_e and velocity V_f .

Having analyzed numerous experimental spectra of cirrus cloud particles, Kosarev and Mazin (1989) found that size distributions of these particles can be satisfactorily described by the gamma function of different orders (usually from 0 to 2). In terms of the diameter D of the equal-volume sphere, these distributions are given by

$$N(D) = N_0 D^n \exp\left[-(3.67 + n) \frac{D}{D_m}\right], \quad (2)$$

where n is the order of the distribution, D_m is the median size that splits the distribution into two equal-

volume parts, and N_0 is the distribution parameter related to particle concentration (see Appendix); D_m represents one of the characteristic sizes of a particle spectrum that can be reformulated into other characteristic sizes, for example, effective or mean sizes. Gamma distributions of different orders n differ from each other by the distribution width.

Sizes of cirrus particles usually do not exceed 2 mm (Kosarev and Mazin 1989; Dowling and Radke 1990), which is still within the Rayleigh regime of scattering for radar frequencies up to Ka-band (Yeh et al. 1982). For Z_i , radar reflectivity with respect to ice and IMC, one can write for spherical particles:

$$Z_i = \int_{D_{\min}}^{D_{\max}} D^6 N(D) dD, \quad (3)$$

and

$$\text{IMC} = \frac{\pi\rho}{6} \int_{D_{\min}}^{D_{\max}} D^3 N(D) dD, \quad (4)$$

where D_{\min} and D_{\max} are the minimum and maximum particle sizes in cloud and ρ is the ice density. Direct microphysical probes of cirrus particles show that minimum and maximum sizes are usually about 5 μm and 2 mm, respectively. Our computational analysis shows that using zero and infinity as the integral limits instead of the values cited above produces differences of only a few percent in the integrals (3) and (4) for $D_m \leq 500 \mu\text{m}$. Thus for simplicity, 0 and ∞ for the integral limits are used further. Integration from 0 to ∞ results in the following equations:

$$Z_i = f_1(n) C D_m^6, \quad (5)$$

$$\text{IMC} = f_2(n) C D_m^3, \quad (6)$$

where C is particle concentration and f_1 and f_2 are known coefficients given in the appendix. Particle fall velocity V_f is the reflectivity-weighted velocity of individual particles, v_f :

$$V_f = \frac{\int_0^{\infty} v_f N(D) D^6 dD}{\int_0^{\infty} N(D) D^6 dD}. \quad (7)$$

Experimental studies of fall velocities of individual ice crystals show that they can be fitted by an expression of the form (Pruppacher and Klett 1978):

$$v_f = A D^B, \quad (8)$$

where A and B are constant for a particular crystal shape. Experimental data on A and B presented by Pruppacher and Klett (1978) show that B varies generally from about 0.75 to 1.4 for different particle shapes and A shows much greater variations that can be as high as two orders of magnitude. Using (8) in (7) and performing the integration gives

$$V_f = Af_3(n, B)D_m^B, \quad (9)$$

where $f_3(n, B)$ is given in the appendix.

Doppler radar measurements give vertical profiles of V_f , so we must account for vertical changes in the V_f - D_m relationship due to changes in air density and viscosity. It is assumed that particle habits do not change significantly through the cloud depth, thus the height dependence can be given by an expression (Pruppacher and Klett 1978):

$$V_f = A \left(\frac{\rho_a}{\rho_{a0}} \right)^{\alpha-1} \left(\frac{\eta_a}{\eta_{a0}} \right)^{1-\alpha} f_3(n, B)D_m^B, \quad (10)$$

where ρ_a and ρ_{a0} , and η_a and η_{a0} are the air density and dynamic viscosity at an arbitrary height and at cloud-bottom levels, respectively. Coefficient α is fairly independent of particle shapes and is about 0.9 for the range of the Reynolds numbers $0.1 \leq N_{Re} \leq 4$ appropriate for most cirrus particles. Air density ρ is height and temperature dependent and dynamic viscosity η is only temperature dependent, so the height dependent part of (10) can be easily calculated if the temperature profile is known.

Radar reflectivity Z_i and fall velocity V_f are the quantities obtained from measurements by vertically pointed Doppler radar at different heights. Assuming the particle distribution (i.e., n), however, there are still four unknowns (i.e., C , D_m , A , and B) and only two measured values (i.e., Z_i and V_f) for each radar range gate. Given relatively low variations of B , the number of unknowns can be reduced to 3 assuming a value for B somewhere in the middle of the region of its variations (e.g., $B = 1$ would be a reasonable choice if there is no a priori information about predominant particle shapes). However, as was pointed out earlier, natural variations of A are much greater than those of B , and A cannot be excluded from the list of unknowns. This requires one additional independent measurement.

This measurement can be obtained from simultaneous measurements of IR radiation of a cloud with an IR radiometer operating in the atmospheric transparency "window." Matrosov et al. (1992) showed that optical thickness τ of a cloud can be estimated from vertical IR brightness temperature measurements and the thermodynamic temperature profile obtained, for example, from radiosonde sounding.

The optical thickness of a cloud can be expressed as follows:

$$\tau = \frac{\pi}{4} \sum_j \left[\int_0^\infty K_e(D) D^2 N(D) dD \right] \Delta h_j, \quad (11)$$

where Δh_j is the radar range gate spacing, K_e is the extinction efficiency, and the summation is performed over all the range gates within a cloud. It was shown by Matrosov et al. (1992) that assuming $K_e = 2$ results in an error in τ that does not exceed about 8% for a

very broad range of D_m from 20 to 600 μm . In this case the integration of (11) yields

$$\tau = \sum_j (f_4(n) C_j D_{mj}^2) \Delta h_j, \quad (12)$$

where again coefficient $f_4(n)$ is given in the appendix.

If the total number of range gates for a radar beam within a cloud is J , the number of input parameters is $2J + 1$, from which there are two vertical profiles of Z_i and V_f and one integral measurement of τ . The number of input parameters corresponds to the number of unknowns, that is, vertical profiles of D_m and C (or IMC), and the coefficient A , which is assumed to be constant over the cloud vertical extent.

The procedure of the retrieval can be formulated as follows. At the first step some initial value A_0 is assumed. Using this value and radar measurements, vertical profiles of particle sizes and concentrations are calculated using (5) and (10). Then (12) is used to calculate the optical thickness τ_0 , which, due to the assumption about A_0 , will differ from the measured value τ . The corrected value A is computed from the initial value A_0 and values of the optical thickness τ and τ_0 ,

$$A = A_0 \left(\frac{\tau}{\tau_0} \right)^{B/4}. \quad (13)$$

The optical thickness calculated with A from (13) coincides with the measured value τ . Equations (5) and (10) are then used again to recalculate the vertical profiles of D_m and C with the corrected value A . Equation (6) gives the vertical profile of IMC from the known vertical profiles of characteristic sizes and concentrations.

Knowing particle sizes, concentrations, and fall velocities, one can calculate some other parameters of cloud microstructure. One such parameter, important in cloud modeling, is ice mass flux (IMF) defined by:

$$\text{IMF} = \frac{\pi \rho}{6} \int_0^\infty D^3 v_f(D) N(D) dD. \quad (14)$$

The result of the integration can be expressed as

$$\text{IMF} = AC f_5(n, B) D_m^{B+3}, \quad (15)$$

where the coefficient $f_5(n, B)$ is given in the appendix.

3. Observational and retrieved data

A dataset collected during the FIRE-II experiment was chosen to illustrate the proposed method for estimating vertical profiles of cirrus cloud microphysical parameters. This large multiagency experiment took place in November–December 1991 in Coffeyville, Kansas, and was specifically designed for studies of cirrus clouds with various remote sensors (NASA 1991). For the purpose of the illustration, the 25–26 Novem-

ber cloud case was chosen. This case was one of the priority cirrus cloud cases during FIRE-II.

Radar data were taken by the WPL Doppler 8.6-mm wavelength (Ka band) radar with the antenna in the zenith position. Radar measurements produced vertical profiles of reflectivity Z_e . Measured effective reflectivities with respect to water, $Z_{e,w}$, were then converted to the reflectivities with respect to ice, Z_i :

$$Z_i = Z_e \frac{|(m_w^2 - 1)(m_w^2 + 2)^{-1}|^2}{|(m_i^2 - 1)(m_i^2 + 2)^{-1}|^2} \approx KZ_e, \quad (16)$$

where m_w and m_i are the complex refractive indices of water and ice, respectively, at the radar wavelength. The coefficient K depends on the ice density: for the solid ice ($\rho = 0.9 \text{ g cm}^{-3}$) $K = 5.28$, for ice with the density $\rho = 0.6 \text{ g cm}^{-3}$, $K = 10.82$.

a. Estimation of particle fall velocities

Besides measurements of vertical profiles of reflectivity, the radar also measured vertical profiles of Doppler velocities V_m . A novel approach was used to extract fall velocities V_f from measured Doppler velocities V_m [see Eq. (1)]. This approach was made possible by the precise velocity estimates obtained with the 8.6-mm radar during FIRE-II; Doppler velocities were measured with an uncertainty of only a few centimeters per second. The approach is based on the assumption that vertical air motion, when averaged over an hour or longer, is negligible compared with typical ice particle fall velocities. Thus, a long average of Doppler velocity profiles closely approximates profiles of reflectivity-weighted particle fall velocities V_f (Orr and Kropfli 1993).

Doppler velocity averaging is performed for small reflectivity intervals to derive reflectivity-fall velocity relationships as a function of height within the cloud. These relationships are determined from power-law functions fit to the data. The averaging interval should not encompass periods of "convective" activity, that is, intervals with relatively strong ($\sim 2 \text{ m s}^{-1}$) but small-scale updrafts or downdrafts. Such infrequent periods are usually apparent by inspection and can easily be removed.

Figure 1 shows the results of applying this approach to the cirrus cloud observed on 26 November 1991. The averages were performed over a 3-h interval for 1-dB-wide reflectivity intervals. The resulting averaged Doppler velocities, that is, estimates of reflectivity-weighted particle fall velocities were plotted against their corresponding reflectivity values. Data are plotted for four different height intervals. Corresponding power-law relationships between reflectivity and fall velocity are also shown. These relationships are then used to estimate vertical profiles of fall velocities at any given time moment within the averaging interval. Such vertical profiles are then used as input information for retrieval of cirrus cloud microphysical properties.

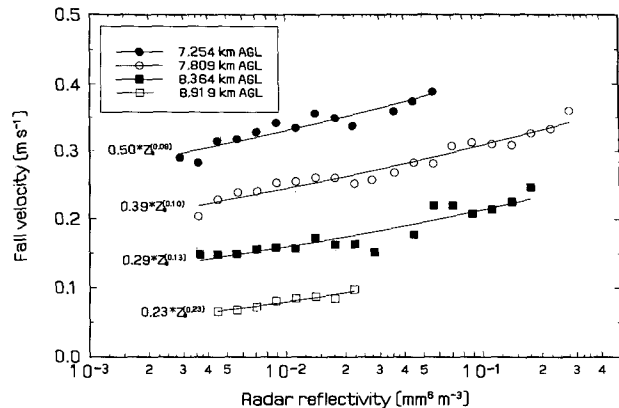


FIG. 1. Particle fall velocity versus reflectivity observed during FIRE-II on 26 November 1991.

One can see that the data for different heights are nicely separated from each other and the standard deviations of data about the best-fit curves are less than 4 cm s^{-1} . Changing the averaging time interval to 2 h does not cause significant variations in estimated values of V_f , which demonstrates the soundness of the approach in this case. Good separation of data for different heights and small values of standard deviations could serve as indicators of applicability of the described procedure to estimate particle fall velocities in other experimental situations.

b. Estimation of cloud optical thickness from IR measurements

The WPL radiometer complex consisted of a narrow-angle IR radiometer that measures downwelling radiation at wavelengths between 9.95 and 11.43 μm and a two-channel microwave radiometer (31.65 and 20.6 GHz). The radiometer site was located about 800 m away from the radar site almost exactly in the downwind direction. Radar VAD (velocity-azimuth display) measurements also indicated that wind speed within the cloud was about 28 m s^{-1} and was relatively constant in speed and direction during the cirrus cloud event from 1830 to 2130 UTC. Radiometers were pointed vertically and 30-s data averaging was used. Likewise, 30-s averaging of radar data was used and a 30-s shift between the radar and radiometer datasets was employed to account for the cloud advection between the systems.

A procedure based on the two-stream radiative transfer model was used to retrieve cloud optical thickness τ (Matrosov et al. 1992). The input information is the ground-level measurement of IR brightness temperatures, the vertical profile of temperature in the cloud, the atmospheric transmittance P_a at "window" frequencies, and the effective temperature T^* of the atmospheric thermal radiation at these frequencies. The latter two values are needed to infer the brightness

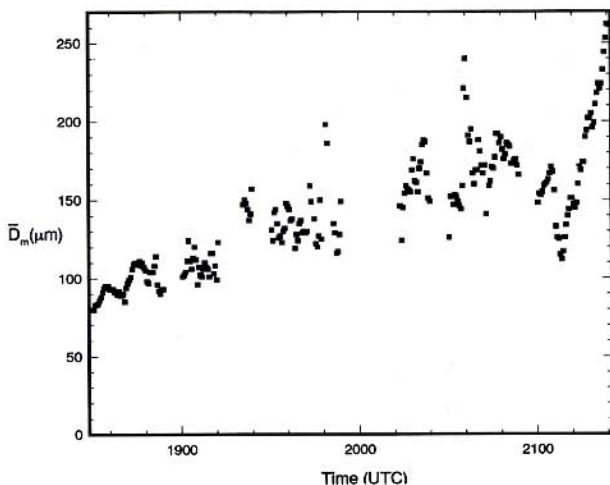


FIG. 2. Retrieved vertically averaged median diameter of cirrus particles during a 3-h period of observation on 26 November 1991.

temperature at the cloud-bottom level T_b from the equation

$$\mathcal{B}(T_{bm}) = \mathcal{B}(T_b)P_a + \mathcal{B}(T^*)(1 - P_a), \quad (17)$$

where T_{bm} is the brightness temperature measured at the ground. In order to calculate T^* , the information on the humidity and temperature vertical profiles is needed. These profiles were taken from the radiosonde launched at 2025 UTC. Atmospheric transmittance P_a is determined mostly by the integrated water vapor amount, which was known from microwave radiometer measurements. For the radiosonde data, estimations yielded values of about 280 K and 0.88 for T^* and P_a , respectively. The changes in water vapor amount measured by the microwave radiometer were accounted for when retrieving values of optical thickness.

We note that the procedure used here for inferring the cloud optical thickness could produce biased results when cloud is very dense ($\tau \geq 3.0$) or very thin ($\tau \leq 0.2$). In such situations some other procedures for estimating τ can be developed. For example, the information on the cloud optical thickness can be potentially obtained using spectral IR measurements near the ozone absorption line at $9.6 \mu\text{m}$. Another way to improve accuracy of the optical thickness retrieval is to use more precise multistream radiative transfer schemes instead of the two-stream model.

c. Retrieved particle sizes and IMC

Figure 2 shows how the median particle sizes \bar{D}_m averaged through the cloud depth changed as the cloud developed from about 1830 UTC, when it began showing continuous radar echoes, to about 2130 UTC, when it became very thick and the microwave radiometer began showing a substantial amount of liquid water. The data on this figure were obtained using the technique described by Matrosov et al. (1992).

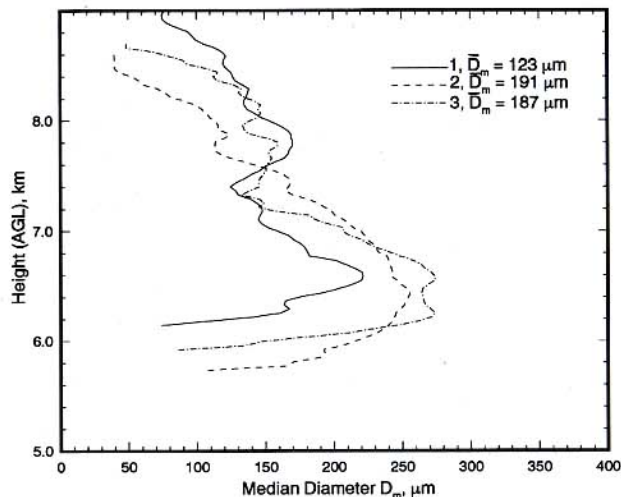


FIG. 3. Retrieved vertical profiles of particle median diameters at 1) 1952, 2) 2047, and 3) 2117 UTC.

When calculating vertical profiles of cloud microstructure parameters using the retrieval technique described in this paper, range gates having fall velocities V_f less than 6 cm s^{-1} were ignored due to possible large relative errors in measuring such low velocities (Orr and Kropfli 1993). Only a few range gates at the cloud top were affected and it did not significantly alter the results of the retrieval, however.

Figures 3 and 4 show the retrieved vertical profiles of the particle median diameter and IMC. The range gate spacing is 37 m. For the purpose of illustration, three profiles at 1952, 2047, and 2117 UTC were chosen because at these times, the infrared and radar properties of the cloud did not change significantly over periods of about 2 min. Also, the cloud geometrical thickness did not change significantly. Such conditions

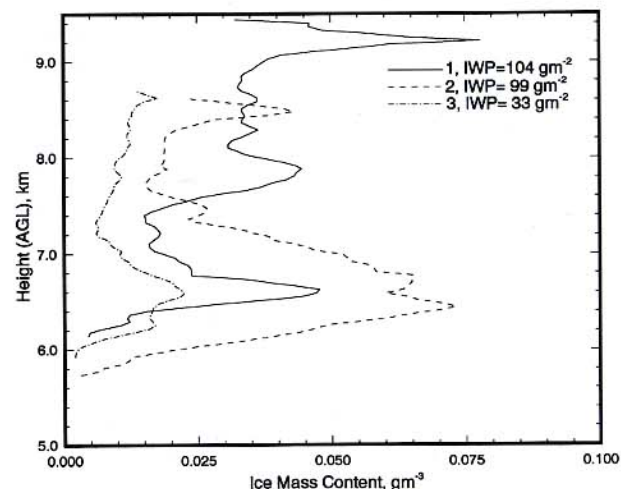


FIG. 4. Same as Fig. 2 but showing IMC vertical profiles.

were chosen to minimize errors introduced by the spatial separation between the radar and IR radiometer even though the correction for the cloud horizontal advection was introduced. Figures 3 and 4 also show the calculated values of IWP and IMC weighted particle sizes \bar{D}_m averaged through the whole vertical extent of the cloud. The presented data were retrieved assuming density of cirrus particles to be 0.8 g cm^{-3} and exponent $B = 1$.

In spite of having similar values of brightness temperatures at 1952 and 2047 UTC, the cloud was apparently quite different microphysically resulting in the significantly different reflectivity values: the mean \bar{Z}_e for 1952 and 2047 UTC were -11.2 and -6 dBZ, respectively. At 2047 UTC, the lower part of the cloud consisted of larger particles at smaller concentrations compared with 1952 UTC. The cloud was much denser in its lower half at 2047 UTC and the maximum values of IMC exceeded 0.05 g m^{-3} . On the other hand, at 1952 UTC, there were three obvious maxima in particle median size and IMC.

The vertical profiles of D_m and IMC retrieved from measurements taken at 2117 UTC show that characteristic sizes of cirrus particles were close to those at 2047 UTC. However, corresponding values of IMC for 2117 UTC were significantly less than ones observed earlier because of smaller particle concentrations. The vertically averaged value for \bar{Z}_e at 2117 UTC was -10.8 dBZ, which is very close to the value for 1952 UTC.

The data presented for these three different time periods demonstrate how microphysically different situations can produce similar values of downwelling IR brightness temperatures or radar reflectivities. Combining measurements from the Doppler radar and the IR radiometer allows us to resolve these ambiguities and get valuable information on microphysical properties of cirrus clouds.

4. Estimation of errors

When formulating the technique, it was assumed that ice particles in cirrus clouds are spherical. In reality, cirrus particles have a great variety of different shapes. Compared with wavelengths in the atmospheric transparency region ($\lambda \sim 11 \mu\text{m}$), cirrus particles are usually large, and, therefore 2 is a good approximation for the extinction efficiency (Matrosov et al. 1992). In this case the difference between extinction coefficients for nonspherical particles and equal-volume spheres is determined by the difference in geometrical cross-sectional areas of the particles. Unlike the situation with the IR radiometer, the radar wavelength ($\lambda = 8.66 \text{ mm}$) is large compared with particle sizes. Backscatter from small nonspherical particles is greater than from equal-volume spheres (Atlas et al. 1953).

In order to estimate the effects of nonsphericity, we assume that particles are either prolate or oblate spheroids. These simple geometrical models were used quite

successfully in describing scattering and extinction properties of nonspherical atmospheric particles (Oguchi 1983). Another justification for using spheroidal models is that the scattering properties for ice crystals of smaller size parameters depend largely on the overall shape but not on the subtle differences in particle structure (Dungey and Bohren 1992; Takano et al. 1992). In addition, according to Sassen (1980), ice crystals tend to be oriented with their major dimensions in the horizontal plane. Consequently, the horizontal orientation of particles was assumed.

Figure 5 shows the backscattering ratio r of horizontally oriented oblate and prolate spheroids to that of equal-volume spheres when viewed vertically with circular polarization (the observational geometry of FIRE-II). The presented calculations were made assuming the ice density to be 0.9 g cm^{-3} and using the Rayleigh approach, which is applicable for almost all cirrus particles at Ka band. The dependencies shown in Fig. 5 were approximated by the power law and produced the following equations:

$$r_o = b^{-0.38}, \quad (18)$$

$$r_p = b^{-0.23}, \quad (19)$$

where b is the particle minor-to-major dimension (aspect ratio) and subscripts o and p stand for oblate and prolate particles, respectively. The error of approximations (18) and (19) is less than 2% when $b \geq 0.2$.

The ratios of geometrical cross sections of spheroidal particles to those of equal-volume spheres are given by

$$s_o = b^{-2/3} \quad (20)$$

$$s_p = b^{-1/3}. \quad (21)$$

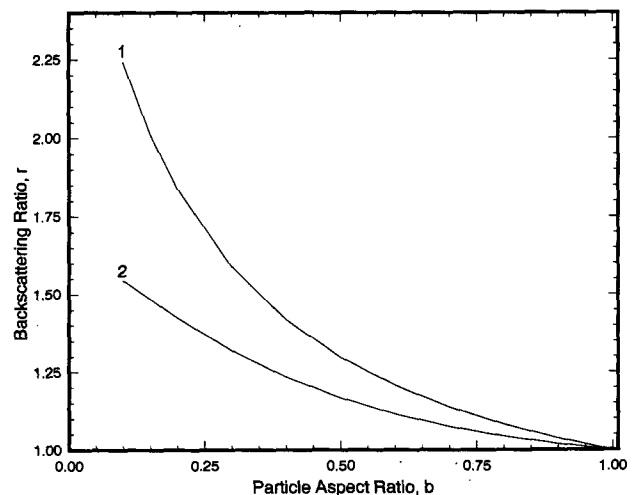


FIG. 5. Ratio of backscattering cross sections of 1) oblate and 2) prolate spheroids to that of equal-volume spheres as a function of the spheroids aspect ratio when viewed vertically.

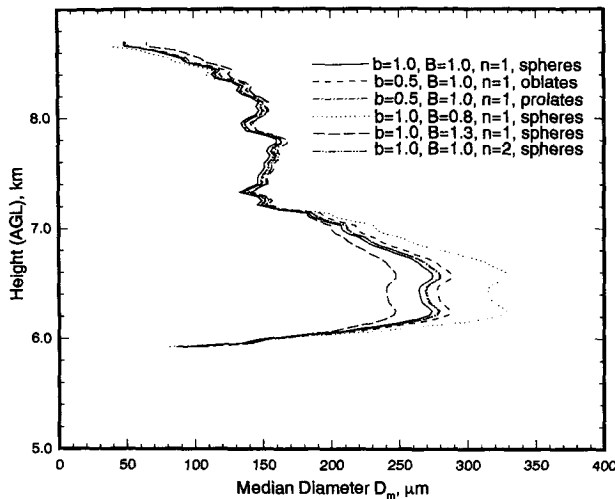


FIG. 6. Vertical profiles of particle median diameters D_m at 2117 UTC computed with different assumed values for particle aspect ratio b , exponent B in the fall velocity–size relationship [Eq. (12)], and the order n of the gamma distribution.

In order to account for nonsphericity, modified values of coefficients $f_1^*(n)$ and $f_4^*(n)$ in (5) and (12) must be used:

$$f_1^*(n) = r_s f_1(n) \quad (22)$$

$$f_4^*(n) = s_s f_4(n), \quad (23)$$

where subscript s (shape) can be either p (prolate) or o (oblate).

Soundings at 2117 UTC were chosen to analyze possible errors in the retrieved results due to different a priori assumptions. Figure 6 shows how retrieved particle sizes D_m would change if particles are assumed to be oblates (curve 2) or prolates (curve 3) with the aspect ratio $b = 0.5$. As one can see, accounting for nonsphericity does not change values of D_m significantly. Variations do not exceed 7%. This can be explained by the fact that accounting for nonsphericity in the extinction (IR) and reflectivity (radar) parts of the problem produces errors of the opposite signs. These errors partially cancel out when retrieving values of D_m .

Curves 4 and 5 in Fig. 6 show the result of the retrieval of D_m if the exponent B in (9) is assumed to be 0.8 (curve 4) or 1.3 (curve 5) rather than 1. The results proved to be quite sensitive to variations in B for large particles with $D_m \geq 200 \mu\text{m}$. The variations in D_m could reach about 20%. For smaller particles variations in retrieved particle sizes due to variations in B are not that great. Note that changes of B from 0.8 to 1.4 cover almost entirely the range of variation of this parameter. High sensitivity of D_m to the exponent B in some way reflects the indirect influence of particle shapes because oblate particles tend to fall slower ($B \leq 1$) and prolate ones faster ($B \geq 1$).

Curve 6 in Fig. 6 shows the results of retrieval assuming that particles are distributed according to the gamma function of the second order ($n = 2$ rather than $n = 1$). As one can see, variations in D_m , due to the order of the gamma distribution, do not exceed a few percent.

Figure 7 shows the results of the IMC retrieval made with different assumptions about particle shapes, the exponent B , and the distribution parameter n . The conditions under which all six curves in Fig. 7 were obtained are the same as in Fig. 6. Retrieved IMC values proved to be more sensitive to a priori assumptions than particle size. This can be explained by the cubic dependence of IMC on D_m and also by higher variability of particle concentration C . Variations in the retrieved individual values of IMC can be as high as 35%. However, integral values of IWP do not show such great variations. For the six cases presented in Fig. 7, values of IWP were 33, 23, 27, 29, 34, and 35 g m^{-2} , respectively, which corresponds approximately to the maximum 30% variation with respect to the value obtained assuming spherical particles with $B = 1$ and $n = 1$.

Figure 8 shows how different assumptions about particle shapes, distributions, and size–fall velocity relationships affect the estimated vertical profile of IMF. The relative errors in IMF due to these assumptions are close to those for IMC. Moreover, the vertical profiles of IMC and IMF look very similar, though the relative strengths of local maxima are different. It can be explained by the fact that dependencies of IMC and IMF on particle sizes and concentrations are similar [see (6) and (15)] though the exponents to which D_m is raised are different.

Variations in the density of ice cause proportional variations in coefficients f_2, f_5 , and K [Eqs. (6), (15), and (16)]. A change in the assumed ice density from

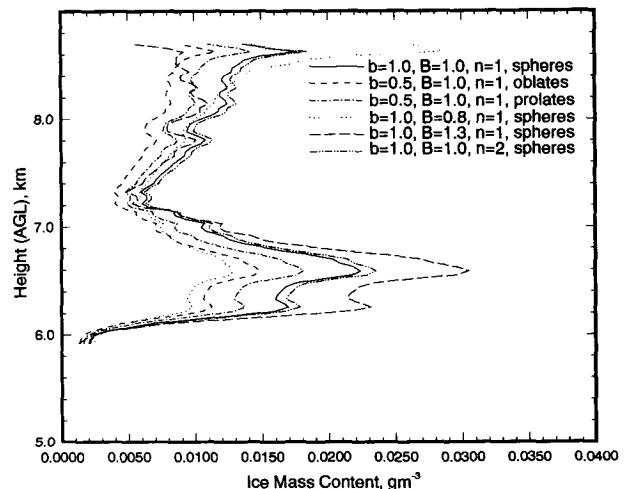


FIG. 7. Same as Fig. 5 but showing the vertical profiles of ice mass content.

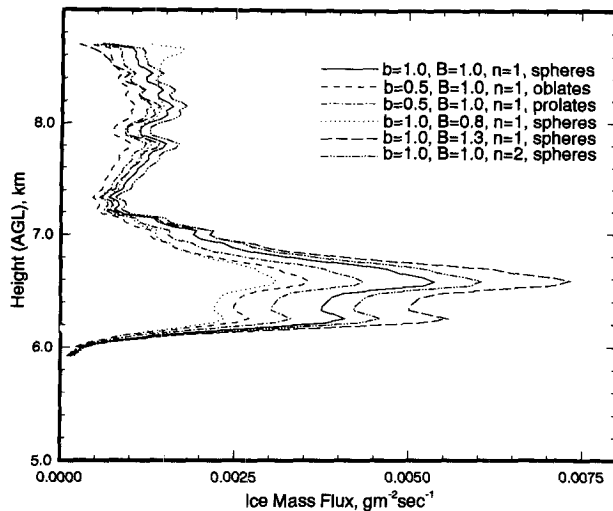


FIG. 8. Same as Fig. 5 but showing the vertical profiles of ice mass flux.

0.9 to 0.6 g cm^{-3} changes the values of D_m , IMC, and IMF by approximately +20%, -20%, and -20%, respectively. These changes do not depend on the absolute values of the microphysical parameters and therefore are not plotted.

In addition to estimating the sensitivity of the retrieval to a priori assumptions, possible errors that could occur because of the uncertainty of input parameters themselves were also evaluated. The error analysis showed that a 1-dB error in radar reflectivities can result in 5%–7% error in both D_m and IMC.

An error of 3 cm s^{-1} in estimating fall velocities V_f , at typical value of 20 cm s^{-1} , produces 7%–9% error in D_m and IMC. We note, however, that this magnitude of velocity error for smaller fall velocity values, usually observed at the cloud top, could result in larger errors of retrieved parameters.

And, finally, 30% error in estimated cloud optical thicknesses can result in errors of about 5% in D_m and about 15% in IMC and IMF.

Summarizing all the sources of errors mentioned above, one can conclude that expected errors of retrieved values of D_m could be of an order 20%–30%. One can expect even higher errors in IMC and IMF.

5. Comparisons

The proposed method to retrieve vertical profiles of cloud microstructure parameters represents a further development of the technique suggested earlier by Matrosov et al. (1992) for inferring particle sizes averaged through cloud depth. Averaging vertical profiles of D_m depicted in Fig. 3 gives the mean values \bar{D}_m 123, 191, and $187 \mu\text{m}$ for the profiles at 1952, 2047, and 2117 UTC, respectively. The corresponding values obtained with the earlier technique (Matrosov et al. 1992) are

129, 192, and $194 \mu\text{m}$, respectively. The values of IWP show greater discrepancies. The proposed method gives, for the three profiles in Fig. 4, the values 104, 99, and 33 g m^{-2} , and the earlier technique by Matrosov et al. (1992) yields the values 118, 110, and 37 g m^{-2} , respectively.

An empirical relationship between IMC and radar reflectivity suggested by Sassen (1987) to calculate values of IWP for the chosen profiles was also used. This relationship, given by the equation [$\text{IMC} (\text{g m}^{-3})$, $Z_i (\text{mm}^6 \text{ m}^{-3})$]

$$\text{IMC} = 0.037Z_i^{0.696}, \quad (24)$$

was computed from measured ice particle size distribution.

For the purpose of convenience, these comparisons are summarized in Table 1. Note that discrepancies in the results of this technique and the previous one (Matrosov et al. 1992) are relatively small, especially for \bar{D}_m , and do not exceed estimated errors of retrieval. This suggests that the earlier technique for estimating mean values \bar{D}_m can be used when information on Doppler velocities is not available or when there is no need for the vertically resolved information about cloud microstructure. For the shown examples, agreement between our results and those obtained from (24) is quite satisfactory given that, unlike this method, (24) does not account for independent variations of particle characteristic sizes and concentrations.

Cirrus particle sizes, retrieved by the proposed method, were also compared with direct in situ measurements. Direct measurements were taken by the balloon-borne ice-crystal replicator (Miloshevich and Heymsfield 1992). Unlike many other particle sensors, the replicator is sensitive to a great dynamic range of particle sizes from about $5 \mu\text{m}$ to the largest sizes occurring in cirrus clouds. The replicator balloon was launched at 2025 UTC from near the radar site. Consideration of the balloon and cloud advection suggests that 2035 UTC is the best time to compare the replicator samples with radar-radiometer measurements.

The cloud at this time was highly changeable in both radar and infrared properties. Figure 9 shows the re-

TABLE 1. Measured and retrieved parameters for three profiles.

| Property | Profile | | |
|--|---------|-------|-------|
| | 1 | 2 | 3 |
| Time (UTC) | 1952 | 2047 | 2117 |
| Brightness temperature (K) | 241.1 | 243.4 | 223.8 |
| Average reflectivity (dBZ) | -11.2 | -6.0 | -10.8 |
| $\bar{D}_m (\mu\text{m})$ (this method) | 123 | 191 | 187 |
| $\bar{D}_m (\mu\text{m})$ (Matrosov et al. 1992) | 129 | 192 | 194 |
| IWP (g m^{-2}) (this method) | 104 | 99 | 33 |
| IWP (g m^{-2}) (Matrosov et al. 1992) | 118 | 110 | 37 |
| IWP (g m^{-2}) [using Eq. (24)] | 67 | 129 | 58 |

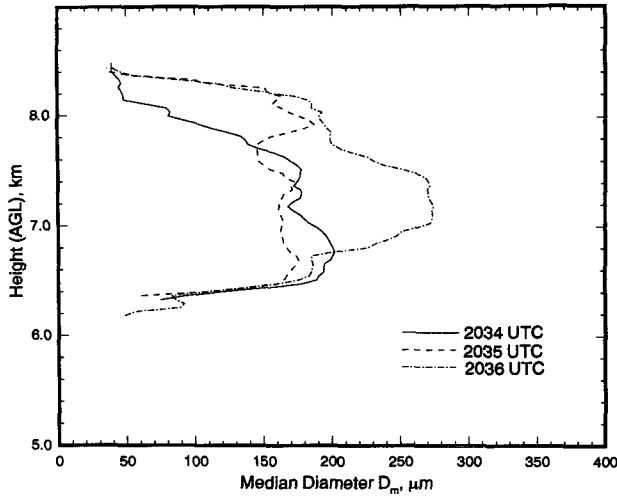


FIG. 9. Vertical profiles of particle median diameters D_m at 2034, 2035, and 2036 UTC.

trieved profiles of D_m for three nearby times: 2034, 2035, and 2036 UTC. The retrieval was done by assuming that exponent $B = 1$ [see (9)]. At an altitude of 7.1 km, the replicator showed for mean maximum dimension of cirrus particles $D_{\max} = 215 \mu\text{m}$ (L. M. Miloshevich and A. J. Heymsfield 1992, personal communication). The particle aspect ratio appeared to be about 0.5. This yields an estimation of the mean diameter of the equal-volume sphere of about $130 \mu\text{m}$.

The data, shown in Fig. 9 for the ice bulk density $\rho_s = 0.8 \text{ g cm}^{-3}$, suggest that the dynamic range for the median diameter of the equal-volume sphere D_m at 7.1 km and around 2035 UTC was from about 170 to 280 μm . Recalculating this range to the mean diameters (assuming the gamma distribution of the first order) gives the corresponding range from about 75 to 130 μm , which is in general agreement with the replicator data. This agreement is good given all the uncertainties of both remote and direct measurements.

6. Conclusions

This paper describes a new method for estimating vertical profiles of cirrus cloud microphysical parameters from ground-based Doppler radar measurements of vertical profiles of reflectivity and Doppler velocities and IR measurements of downwelling radiation in the atmospheric transparency region (10–12 μm). The microphysical parameters of interest are the median equal-volume diameters of cirrus particles IMC (or particle concentration), and IMF in each radar range gate. Estimated values of IMC allow one to calculate IWP—a parameter that is important in evaluating cloud impact on the planetary radiation budget. The proposed method represents the further development of an earlier technique by Matrosov et al. (1992) for estimating characteristic particle sizes and concentra-

tions averaged through the cloud depth. Vertically averaged particle sizes and IWP values obtained with the new and old methods are in reasonable agreement.

Studies of the retrieval accuracy reveal that the major error source is uncertainty in the particle fall velocity–size relationships. A possible error of the estimation of characteristic sizes, IMC, and IMF due to assumptions and measurement errors, could reach about 40%. The method was applied to data obtained on 26 November 1991 during FIRE-II.

Acknowledgments. The authors would like to thank L. M. Miloshevich and A. J. Heymsfield for providing the particle size information from the replicator sample. B. W. Bartram and K. A. Clark were responsible for the performance of the WPL Ka-band radar. This work was funded, in part, by the U.S. Department of Energy's Atmospheric Radiation Measurement Program under Grant DE-AI06-91RL12089 and by the NOAA Climate and Global Change Program Office.

APPENDIX

Derivation of Coefficients f_k ($k = 1, \dots, 5$)

Coefficients $f_k(n)$ ($k = 1, \dots, 5$) in Eqs. (5), (6), (10), (12), and (15) depend on the particle size distribution. For the gamma distribution of different orders n they can be easily obtained by size integration of the corresponding equations. If the lower limit and the upper limit in these integrals (D_{\min} and D_{\max}) are assumed to be zero and infinity, respectively, the integration yields:

$$f_1(n) = \frac{\Gamma(n+7)}{\Gamma(n+1)(3.67+n)^6}, \quad (\text{A1})$$

$$f_2(n) = \frac{\rho \pi \Gamma(n+4)}{6\Gamma(n+1)(3.67+n)^3}, \quad (\text{A2})$$

$$f_3(n, B) = \frac{\Gamma(n+7+B)}{\Gamma(n+7)(3.67+n)^B}, \quad (\text{A3})$$

$$f_4(n) = \frac{\pi \Gamma(n+3)}{2\Gamma(n+1)(3.67+n)^2}, \quad (\text{A4})$$

$$f_5(n, B) = \frac{\pi \rho \Gamma(n+4+B)}{6\Gamma(n+1)(3.67+n)^{B+3}}, \quad (\text{A5})$$

where ρ is the ice density and Γ is the gamma function. When deriving (A1)–(A5) we used the expression for the total concentration C obtained when integrating (2):

$$C = \frac{N_0 \Gamma(n+1) D_m^{n+1}}{(3.67+n)^{n+1}}. \quad (\text{A6})$$

If we assume a more reasonable value for $D_{\max} \approx 2$ mm, values of the coefficients f_1 – f_5 would be slightly different from those given by (A1)–(A5) and would also slightly depend on D_m . If D_m changes from 20 to

500 μm , changes in these coefficients do not exceed 2%, however, and can be neglected.

REFERENCES

- Atlas, D. M., M. Kerker, and W. Hitschfeld, 1953: Scattering and attenuation by non-spherical atmospheric particles. *J. Atmos. Terr. Phys.*, **3**, 108–119.
- Dowling, D. R., and L. F. Radke, 1990: A summary of the physical properties of cirrus clouds. *J. Appl. Meteor.*, **29**, 970–987.
- Dungey, C. E., and C. F. Bohren, 1992: Backscattering by nonspherical hydrometeors as calculated by the coupled-dipole method: An application in radar meteorology. *J. Atmos. Oceanic Technol.*, **10**, 526–532.
- Ebert, E. E., and J. A. Curry, 1992: A parameterization of ice cloud optical properties for climate models. *J. Geophys. Res.*, **97**, 3831–3836.
- Intrieri, J. M., G. L. Stephens, W. L. Eberhard, and T. Uttal, 1993: A method for determining cirrus cloud particle sizes using lidar and radar backscatter technique. *J. Appl. Meteor.*, **32**, 1074–1082.
- Kosarev, A. L., and I. P. Mazin, 1989: Empirical model of physical structure of the upper level clouds of the middle latitudes. *Radiation Properties of Cirrus Clouds*, Nauka, 29–52.
- Liao, L., and K. Sassen, 1992: Theoretical investigation of the relationship between ice mass content and K_a -band radar reflectivity factor. Preprints, *11th Int. Conf. on Cloud Physics and Precipitation*, Montreal, Amer. Meteor. Soc., 1005–1008.
- Matrosov, S. Y., T. Uttal, J. B. Snider, and R. A. Kropfli, 1992: Estimation of ice cloud parameters from ground-based infrared radiometer and radar measurements. *J. Geophys. Res.*, **97**, 11 567–11 574.
- Miloshevich, L. M., and A. J. Heymsfield, 1992: Microphysical measurements in cirrus clouds from ice crystal replicator sondes launched during FIRE-II. Preprints, *11th Int. Conf. on Cloud Physics and Precipitation*, Montreal, Amer. Meteor. Soc., 525–528.
- NASA, 1991: FIRE cirrus intensive field observations—II: Operations plan. FIRE Project Office and FIRE Cirrus Working Group, NASA/LARC, 116 pp. [Available from Langley Research Center, Hampton, VA 23665-5225.]
- Oguchi, T., 1983: Electromagnetic wave propagation and scattering in rain and other hydrometeors. *Proc. IEEE*, **71**, 1029–1078.
- Orr, B. W., and R. A. Kropfli, 1993: Estimation of cirrus particle fallspeeds from vertically pointing Doppler radar. Preprints, *26th Int. Conf. on Radar Meteorology*, Norman, OK, Amer. Meteor. Soc., 588–590.
- Parol, F., J. C. Buriez, G. Brogniez, and Y. Fouquart, 1991: Information content of AVHRR channels 4 and 5 with respect to the effective radius of cirrus cloud particles. *J. Appl. Meteor.*, **30**, 973–984.
- Pruppacher, H. R., and J. D. Klett, 1978: *Microphysics of Clouds and Precipitation*. D. Reidel, 714 pp.
- Sassen, K., 1980: Remote sensing of planar ice crystal fall altitudes. *J. Meteor. Soc. Japan*, **58**(5), 422–429.
- , 1987: Ice cloud content from radar reflectivity. *J. Climate Appl. Meteor.*, **26**, 1050–1053.
- Stephens, G. L., S. C. Tsay, P. W. Stackhouse Jr., and P. J. Flatau, 1990: The relevance of the microphysical and radiative properties of cirrus clouds to climate and climatic feedback. *J. Atmos. Sci.*, **47**, 1742–1753.
- Takano, Y., K. N. Liou, and P. Minnis, 1992: The effects of small ice crystals on cirrus radiative properties. *J. Atmos. Sci.*, **49**, 1487–1493.
- Uttal, T., and J. Intrieri, 1993: Comparison of cloud boundaries measured with 8.6 mm radar and 10.6 μm lidar. Preprints, *Topical Symp. on Combined Optical-Microwave Earth and Atmosphere Sensing*, Albuquerque, NM, IEEE Geoscience and Remote Sensing Society, 207–210.
- Yeh, C., R. Woo, A. Ishimaru, and J. Armstrong, 1982: Scattering by single ice needles and plates at 30 GHz. *Radio Sci.*, **17**(6), 1503–510.